JOURNAL OF GEOPHYSICAL RESEARCH, VOL. 113, A12206, doi:10.1029/2008JA013237, 2008

Observations of chorus at Saturn using the Cassini Radio and Plasma Wave Science instrument

G. B. Hospodarsky,[1] T. F. Averkamp,[1] W. S. Kurth,[1] D. A. Gurnett,[1] J. D. Menietti,[1] O. Santolik,[2,3] and M. K. Dougherty[4]

Received 1 April 2008; revised 7 July 2008; accepted 7 August 2008; published 6 December 2008.

[1] Observations at Saturn of whistler mode chorus emissions have been obtained by the Cassini Radio and Plasma Wave Science instrument. Data from the first 45 orbits are analyzed, and the characteristics of the chorus emissions are discussed. Wave normal and Poynting vector measurements from the five-channel waveform receiver are used to examine the propagation characteristics of the chorus, and high-resolution measurements from the wideband receiver are used to examine the fine structure. At Saturn, two different types of chorus are detected. The most common observations are of chorus propagating away from Saturn's magnetic equator, suggesting a source near the magnetic equator. This chorus is usually detected for many hours, is only observed below half the electron cyclotron frequency, and occurs primarily from *L* shells of about 5 to 8, and the occurrence of the emission shows no obvious correlation with Saturn magnetic latitude, longitude, or local time. The high-resolution measurements show that the fine structure of this chorus typically consists of larger time scale features (many seconds to minutes) than detected at the Earth (<1 s). The second region of chorus detected at Saturn is in association with local plasma injections. For many of the plasma injection events, chorus emissions are detected both above and below half the electron cyclotron frequency, with a gap in the emission at half the cyclotron frequency. This chorus also shows fine structure at smaller time scales (<1 s to a few seconds), and the overall structure of this chorus appears more similar to chorus detected at the Earth.

Citation: Hospodarsky, G. B., T. F. Averkamp, W. S. Kurth, D. A. Gurnett, J. D. Menietti, O. Santolik, and M. K. Dougherty (2008), Observations of chorus at Saturn using the Cassini Radio and Plasma Wave Science instrument, *J. Geophys. Res.*, *113*, A12206, doi:10.1029/2008JA013237.

1. Introduction

[2] Chorus is an electromagnetic wave emission that propagates in the right-hand polarized whistler mode and has been detected at the Earth, Jupiter, Saturn, Uranus, Neptune, and the Jovian moon Ganymede. Chorus detected at the Earth often consists of rising tones in frequency with fine structure of less than one second [*Gurnett and O'Brien*, 1964; *Burtis and Helliwell*, 1969; *Dunckel and Helliwell*, 1969]. These rising tones occur in the audio frequency range and when recorded in a receiver, sound like the dawn chorus of birds, which gives these waves their name. Chorus is one of the most common and intense whistler mode emissions observed in the Earth's magnetosphere and is believed to be generated by nonlinear interactions of whistler mode waves with energetic electrons [*Storey*, 1953; *Allcock*, 1957; *Helliwell*, 1969]. Chorus at the Earth ranges in frequency from a few hundred Hz to a few kHz, and usually occurs in two distinct frequency bands separated by a gap at one-half the electron cyclotron frequency, f_{ce} [*Tsurutani and Smith*, 1974], with the lower band ranging from about 0.1 to 0.5 f_{ce}, and the upper band from about 0.5 to 0.8 f_{ce} [*Meredith et al.*, 2001]. Chorus often contains complicated fine structure including rising and falling tones, and short impulsive bursts with time scales of much less than a second [*Burton and Holzer*, 1974; *Cornilleau-Wehrlin et al.*, 1978; *Hayakawa et al.*, 1990; *Sazhin and Hayakawa*, 1992; *Lauben et al.*, 1998, 2002; *LeDocq et al.*, 1998; *Santolik et al.*, 2003, 2004]. The origin of this fine structure and its relationship to the source region of chorus is an active area of research [*Inan et al.*, 2004, *Chum et al.*, 2007, *Breneman et al.*, 2007, *Omura et al.*, 2008, and references therein]. At the Earth, chorus is often observed during periods of disturbed magnetospheric conditions [*Tsurutani and Smith*, 1974, 1977; *Inan et al.*, 1992; *Lauben et al.*, 1998] and the occurrence of chorus is associated with energetic (10 to 100 keV), anisotropic ($T_\perp/T_\parallel > 1$) electron

[1]Department of Physics and Astronomy, University of Iowa, Iowa City, Iowa, USA.
[2]Faculty of Mathematics and Physics, Charles University, Prague, Czech Republic.
[3]Institute of Atmospheric Physics, Czech Academay of Sciences, Prague, Czech Republic.
[4]Blackett Laboratory, Department of Space and Atmospheric Physics, Imperial College London, London, UK.

0148-0227/08/2008JA013237$09.00

distributions [*Burton*, 1976; *Anderson and Maeda*, 1977; *Tsurutani et al.*, 1979; *Isenberg et al.*, 1982; *Sazhin and Hayakawa*, 1992]. This association between the particles and the chorus is consistent with a cyclotron resonance interaction generating the waves [*Kennel and Petschek*, 1966; *Curtis*, 1978; *Sazhin and Hayakawa*, 1992].

[3] The chorus is believed to be generated near the terrestrial magnetic equator [*Helliwell*, 1969], and various studies have examined the propagation characteristics of the chorus emissions [*Burton and Holzer*, 1974; *Goldstein and Tsurutani*, 1984; *Hayakawa et al.*, 1984; *Nagano et al.*, 1996; *LeDocq et al.*, 1998; *Hospodarsky et al.*, 2001; *Lauben et al.*, 2002; *Santolik et al.*, 2005]. *LeDocq et al.* [1998] studied simultaneous measurements of all six components of the electric and magnetic field of chorus at a very high rate with the Polar spacecraft. From these measurements, it was determined that the chorus observed by Polar was propagating away from the equator, implying that it is generated very close to the magnetic equator. More recent work with both the Polar and the Cluster spacecraft [*Parrot et al.*, 2003; *Santolik and Gurnett*, 2003; *Santolik et al.*, 2004, 2005] have confirmed these results and have shown that the chorus source region (measured along the magnetic field lines) is a few thousand km in size, and about 100 km transverse to the magnetic field [*Santolik and Gurnett*, 2003; *Santolik et al.*, 2004, 2005]. Although chorus has been studied for many years, the exact details of the source region, the generation mechanism, and the wave-particle interactions are still areas of great interest and recent advances, both with observations and theoretical models [see, e.g., *Horne et al.*, 2003, 2005; *Omura and Summers*, 2006; *Bortnik and Thorne*, 2007; *Katoh and Omura*, 2007; *Summers et al.*, 2007].

[4] Chorus at Saturn was first detected during the Voyager 1 and 2 flybys [*Gurnett et al.*, 1981; *Scarf et al.*, 1982, 1983, 1984]. Because of the flyby geometry, the Voyager spacecraft detected only a few short periods of chorus, and the amount of high-resolution wideband data that was obtained during the flybys was greatly limited owing to telemetry constraints (see *Scarf et al.* [1983] for a discussion of these issues). Furthermore, the lack of a search coil magnetometer and the Voyager plasma wave instrument response to dust impacts in the equatorial region complicates the identification of chorus and other whistler mode waves in the lower-resolution low-rate data. However, a wideband frame was obtained when chorus was present during the Voyager 1 flyby [*Scarf et al.*, 1983]. This high-resolution data showed a band of chorus present below 1/2 f_{ce} (from about 0.2 to 0.4 f_{ce}). The chorus was primarily hiss-like with some rising structures, but the temporal variations were ''unusually slow'' [*Scarf et al.*, 1983]. No chorus above 1/2 f_{ce} was detected by Voyager.

[5] The presence of chorus at Saturn suggests the possibility of wave-particle interaction and pitch angle scattering of the electrons in Saturn's inner magnetosphere. *Scarf et al.* [1983, 1984] examined the chorus detected by Voyager, and found that the amplitudes were too small to play an important role as pitch angle scatterers. However, during the period of the Voyager flybys the magnetosphere of Saturn was not very active, and it is possible that the chorus emission would play a more significant role during more active periods [*Kurth and Gurnett*, 1991].

[6] The Cassini mission to Saturn, owing to its many orbits and the opportunity to sample many different regions of the magnetosphere, allows a much more detailed study of chorus and other plasma waves to be accomplished. This paper examines the observations of chorus in Saturn's magnetosphere obtained by the Cassini spacecraft for the first 45 orbits. The general characteristics and the fine-scale structure of the Saturnian chorus is discussed, and the propagation characteristics of the chorus is presented. The possible correlation between the occurrence of the chorus emission with local time and magnetic latitude is examined, and an initial survey of the amplitudes of the chorus is presented and compared to chorus detected at the Earth and Jupiter.

2. Cassini RPWS Instrument Description

[7] The Cassini Radio and Plasma Wave Science (RPWS) instrument consists of five receivers, a Langmuir Probe, three electric antennas used here as a combination of a dipole antenna (Ex) and an orthogonal monopole antenna (Ew), and a triaxial search coil magnetometer (see *Gurnett et al.* [2004] for a detailed description of the instrument). The receivers cover a range from ~1 Hz to 16 MHz for electric fields, and ~1 Hz to 12 kHz for magnetic fields. This study will primarily use the medium frequency receiver (MFR), the wideband receiver (WBR), and the five-channel waveform receiver (WFR). The MFR sweeps from 24 Hz to 12 kHz, with 80 frequency steps in three bands. A complete spectrum is obtained every 32 s, with the choice of the antenna usually alternating between the Ex electric antenna and the Bz magnetic antenna. The WBR obtains waveforms from one sensor (usually the Ex electric antenna) in one of two frequency bands, either 60 Hz to 10.5 kHz, or 800 Hz to 75 kHz. The duty cycle of the WBR ranges from nearly continuous to a few snapshots per day depending on the telemetry available. For this study, the 60 Hz to 10.5 kHz filter mode is primarily used. The WFR obtains simultaneous waveforms from up to five sensors in one of two frequency bands, either 1 to 26 Hz, or 3 Hz to 2.5 kHz. When two electric and three magnetic antennas are used, polarization and wave normal vector measurements can be obtained and, in certain conditions, the Poynting vector can be determined. The WFR is usually operated with the Ex dipole, Ew monopole, and the three search coil magnetometers (Bx, By, Bz). Usually a 2048-sample waveform, with a 140 μS sample period, is captured every 48 or 320 s in the high-frequency filter mode. This produces a waveform ~0.29 s long, with a gap of 47.71 or 319.71 s until the start of the next waveform.

[8] The simultaneous measurement of five components of the electric and magnetic field by the WFR allows the wave normal and Poynting vector of various low-frequency plasma waves to be determined in many cases. The wave normal vector determines the direction of propagation of a wave, and is important in determining the polarization, the mode, and the source region of the wave. It can also be used to calculate the dispersion relation, to determine various resonances, to estimate the index of refraction, and is helpful in examining wave-particle interactions. The Poynting flux

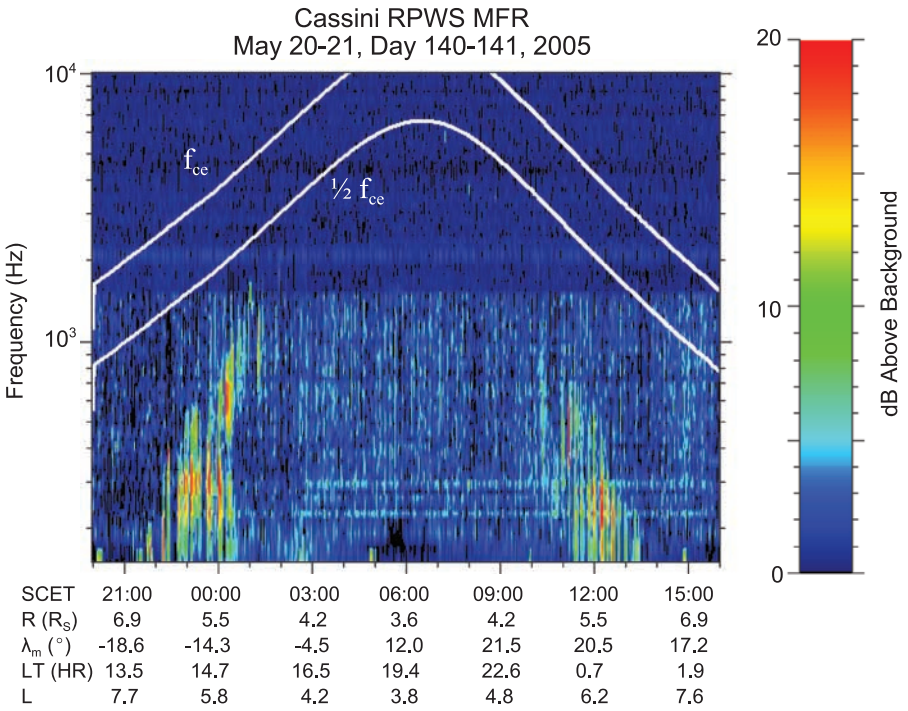

Figure 1. An overview of the magnetic field spectrum observed by the Cassini RPWS medium frequency receiver (MFR) during periapsis of orbit 8. The "magnetospheric" chorus emissions are observed during the inbound trajectory from about day of year (DOY) 140 2100 to DOY 141 0130 Spacecraft Event Time (SCET) and during the outbound trajectory from about DOY 141 1030 to 1400 SCET. The white lines show the electron cyclotron frequency, f_{ce} (top line) and 1/2 f_{ce} (bottom line), that was determined from the magnitude of the magnetic field provided by the Cassini Magnetometer Team.

determines the direction of propagation of the wave energy, and is also helpful in determining the wave mode and the wave generation region.

3. Method of Analysis for the WFR

[9] In this study, the Means method [*Means*, 1972], using code developed by *LeDocq* [1998] for the Polar PWI instrument, and modified for the Cassini RPWS instrument WFR data, is used to determine the wave normal vector, **k**. This method involves computing a spectral matrix that consists of the auto- and cross-power spectra from the three magnetic components. Although this method has an inherent 180° ambiguity in the wave normal direction, this ambiguity can be removed if the Poynting vector, **S**, can be determined. Since the wave normal vector must have a component in the direction of the energy flow, $\mathbf{S} \cdot \mathbf{k}$ must be greater than 0. Because the Cassini WFR only measures five components of electromagnetic waves (two electric and three magnetic), the Poynting vector cannot be determined directly. However, *Shawhan* [1970] showed that for electromagnetic waves below the electron cyclotron frequency, f_{ce}, the missing component can usually be estimated from the five measured components, and the Poynting vector can be determined with good accuracy using $\mathbf{S} = (1/2)\,\mathrm{Re}\{\mathbf{E}(f) \times \mathbf{H}^*(f)\}$, where * indicates the complex conjugate, Re is the real part, and **E**(f) and **H**(f) are the Fourier transforms of the electric and magnetic field waveforms. See *Hospodarsky et al.* [2001] for a more detailed discussion of this analysis method.

4. Chorus Observations at Saturn with Cassini

[10] Figure 1 shows a 20-h magnetic field spectrogram obtained from the Bz search coil magnetometer attached to the medium frequency receiver (MFR) for the period around periapsis of orbit 8. The white lines on Figure 1 show the electron cyclotron frequency, f_{ce} (upper line) and 1/2 f_{ce} (lower line) that was determined from the magnitude of the magnetic field provided by the Cassini Magnetometer Team (MAG) [*Dougherty et al.*, 2004]. During this orbit, chorus is observed both during the inbound trajectory from about 2005, day of year (DOY) 140 2100 to DOY 141 0130 Spacecraft Event Time (SCET), and during the outbound trajectory from about DOY 141 1030 to 1400 SCET. The magnetic field spectrum is shown instead of the electric field spectrum since it most easily shows the electromagnetic chorus emissions and avoids any confusion with the many electrostatic emissions detected in this region. As can be seen, the center frequency of the chorus band increases as f_{ce} increases, and no emission is detected above 1/2 f_{ce} during this period. The majority of the chorus detected at Saturn is similar to this example.

[11] The results of the wave normal and Poynting vector determination of the chorus from Figure 1 is shown in Figure 2. The top two panels show the sum of the electric and magnetic field spectral densities (V^2/m^2Hz and nT^2/Hz) from each of the sensors, with intensity indicated by the

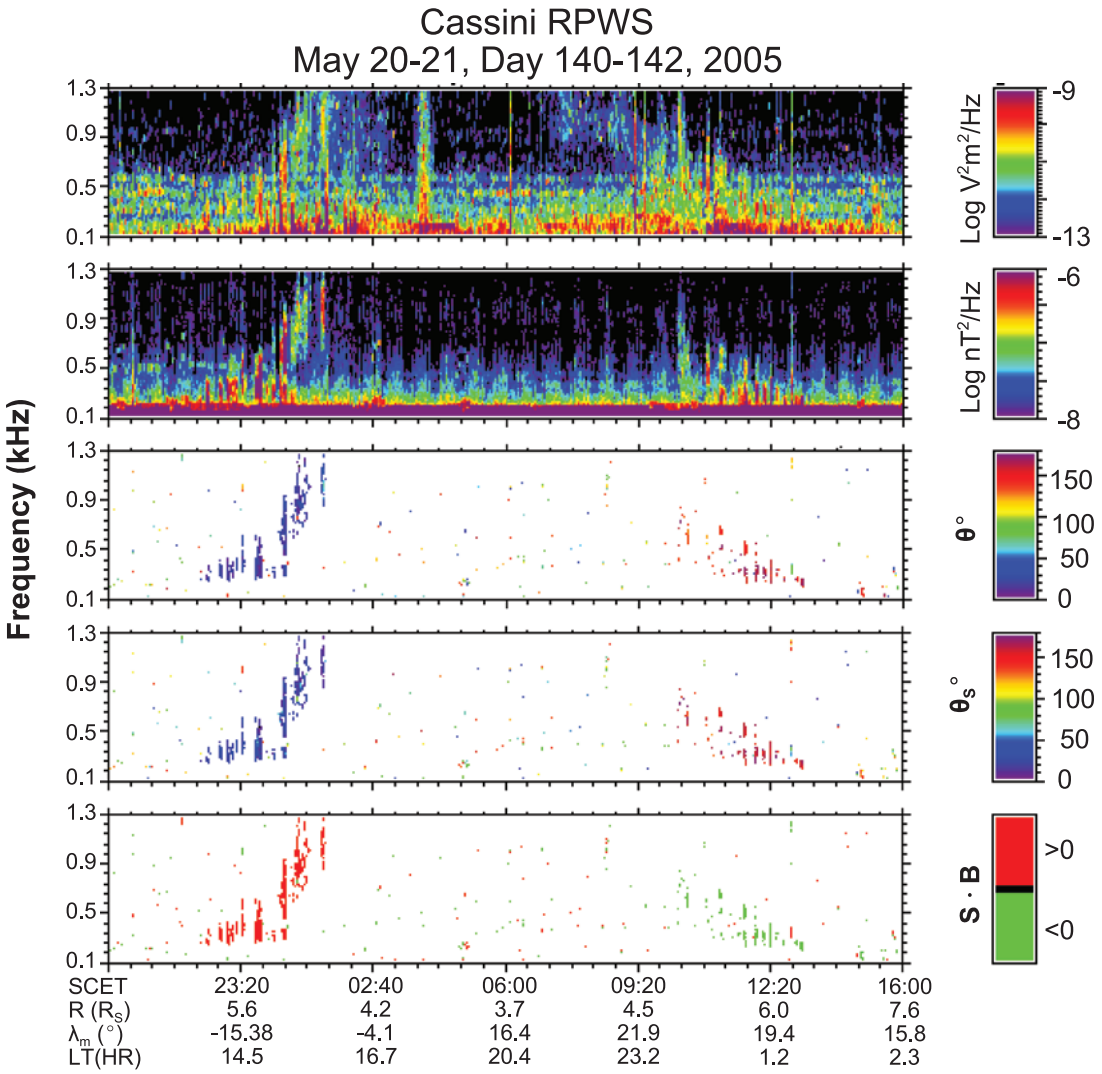

Figure 2. A summary of the waveform receiver (WFR) observations of the wave normal and Poynting vector direction of chorus emissions shown in Figure 1. The top two panels show the sum of the electric and magnetic field spectral density in units of V^2/m^2Hz and nT^2/Hz. The third panel shows the angle, θ_k, between the wave normal vector and the local magnetic field (60-s averaged magnetic field data). The fourth panel shows the angle, θ_S, between the Poynting vector and the ambient magnetic field. The fifth panel shows the sign of the z component of the Poynting vector, $S_z = \mathbf{S} \cdot \mathbf{B_o}$, where $\mathbf{B_o}$ is a unit vector parallel to the magnetic field.

color bar to the right. The third panel shows the angle, θ_k, between the wave normal vector and the local magnetic field (60-s averaged magnetic field data), with the color bar denoting angular values ranging from 0° to 180°. The fourth panel shows the angle, θ_S, between the Poynting vector and the ambient magnetic field, with the color bar denoting angular values ranging from 0° to 180°. The fifth panel shows the sign of the z component of the Poynting vector, $S_z = \mathbf{S} \cdot \mathbf{B_o}$ where $\mathbf{B_o}$ is a unit vector parallel to the magnetic field. When S_z is positive, the Poynting vector has a component in the $+\mathbf{B_o}$ direction, and the emission is plotted in red. When S_z is negative, the Poynting vector has a component in the $-\mathbf{B_o}$ direction, and the emission is plotted in green.

[12] Figure 2 shows that the wave normal and Poynting vector are nearly aligned with the local magnetic field for most of this event. Although it is not shown in Figure 2, the analysis also showed that the chorus is right-hand polarized. The bottom panel of Figure 2 shows that during the inbound period, the chorus is propagating parallel to the local magnetic field (southward and away from the magnetic equator), and during the outbound period, the chorus is propagating anti-parallel to the local magnetic field (northward and away from the magnetic equator), in agreement with *LeDocq et al.* [1998] and *Hospodarsky et al.* [2001] results for chorus at the Earth.

[13] High-resolution WBR observations of chorus from Cassini show that the chorus emissions contain a range of fine structure. For example, Figure 3a shows an approximately 90 s WBR snapshot obtained during the outbound period of Orbit 8 (see Figure 1). The chorus emission in this example is the hiss-like signal from about 250 Hz to 700 Hz.

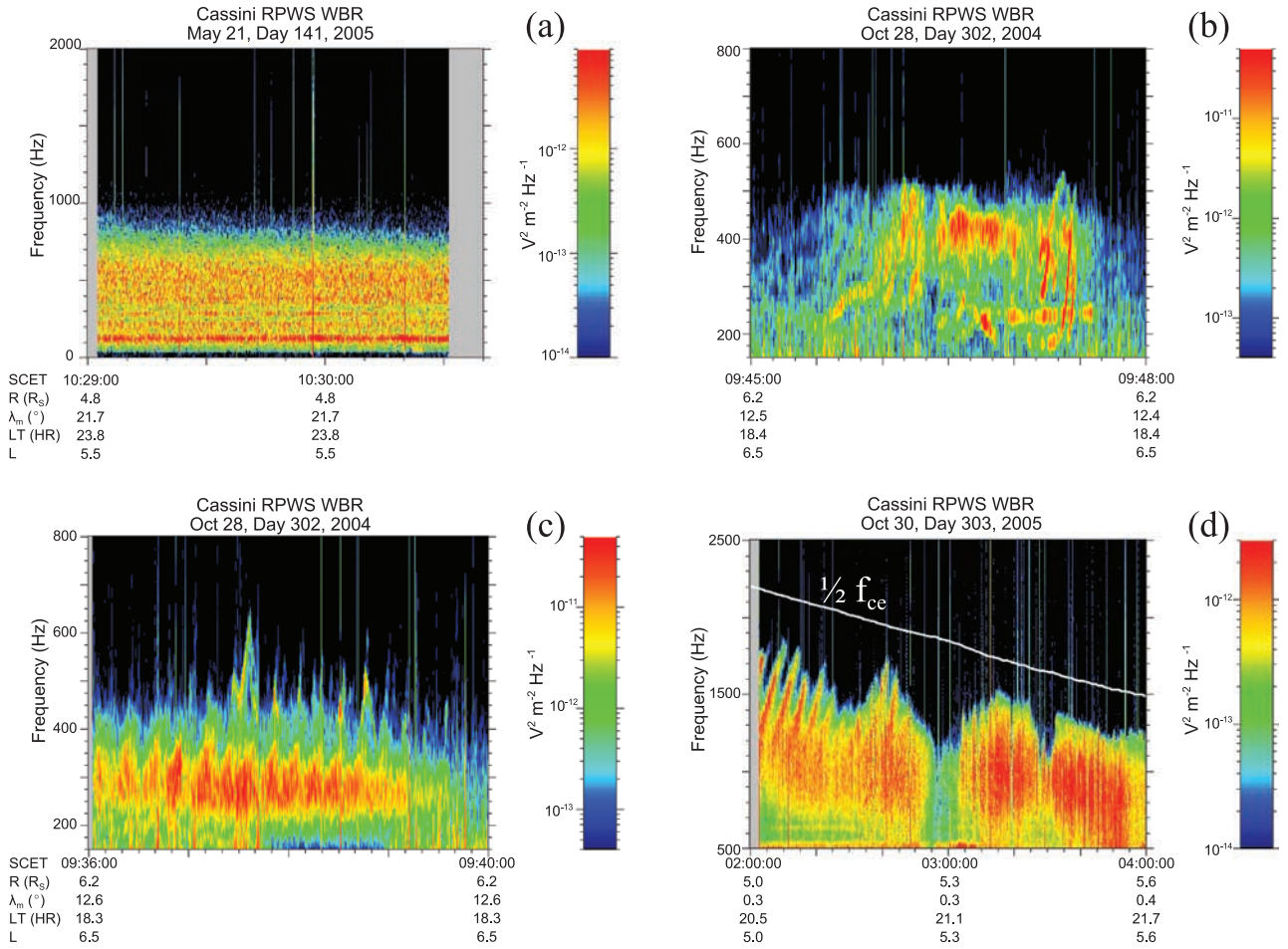

Figure 3. High-rate wideband receiver (WBR) time-frequency spectrograms of the "magnetospheric" chorus emission. The emission is often hiss-like but also shows a variety of fine structure, including narrowband rising tones with time scales on the order of seconds to minutes.

The narrowband lines below about 300 Hz are interference from the Reaction Wheel Assembly (RWA) altitude control system, and are not related to the chorus emission. Figures 3b and 3c show examples of chorus from Orbit A which contain rising-tone fine structure on top of the hiss-like component. Figure 3b shows 3 min of WBR data during a chorus burst that has rising tone-like structures from about 200 Hz to 500 Hz, with rising times ranging from seconds to tens of seconds, on top of a bursty, hiss-like band from about 350 to 450 Hz. Figure 3c shows 4 min of WBR data obtained a few minutes before the example shown in Figure 3b. This burst of chorus shows a series of periodic, broader rising tones from about 200 Hz to 400 Hz, with a period of about 15 s, and a series of much narrower tones from about 400 Hz to 650 Hz. These higher-frequency tones appear to be related to the high-frequency parts of the periodic signature, and both rise and fall in frequency with time. Figure 3d shows 2 h of WBR data obtained during Orbit 17. During the beginning of this period, the chorus consists of a hiss-like component at lower frequencies and a component made up of broadband rising tones with periods of about 6 min rising out of this lower-frequency component. As Cassini moves outbound from Saturn during this period, the chorus drops in frequency and the rising tones appear to merge with the lower-frequency hiss-like component. The white line in Figure 3d shows 1/2 f_{ce} as determined by the MAG. As can be seen, the chorus emissions for this period are always below 1/2 f_{ce}. It should be noted that for Figures 3a, 3b, and 3c, 1/2 f_{ce} is not plotted because it was above the upper frequency limit of the spectrogram.

[14] The majority of the chorus detected at Saturn is similar to the examples discussed above, and has the following characteristics. First, it is always detected below 1/2 f_{ce} and often below 1/4 f_{ce} (the lack of a frequency component above 1/2 f_{ce} also results in the lack of a gap in the emissions at 1/2 f_{ce}). Second, it is usually observed for many minutes to hours, and is observed over a range of magnetic latitude and L shells. Third, the chorus at Saturn contains less fine structure than is often observed with chorus at the Earth, and the fine structure that is observed tends to have longer time scales (seconds to minutes) than chorus detected at the Earth (often fractions of seconds to seconds). Fourth, the chorus propagates away from the magnetic equator, implying that the source region is near the magnetic equator. This type of chorus emission will be called "magnetospheric" chorus for the rest of this paper.

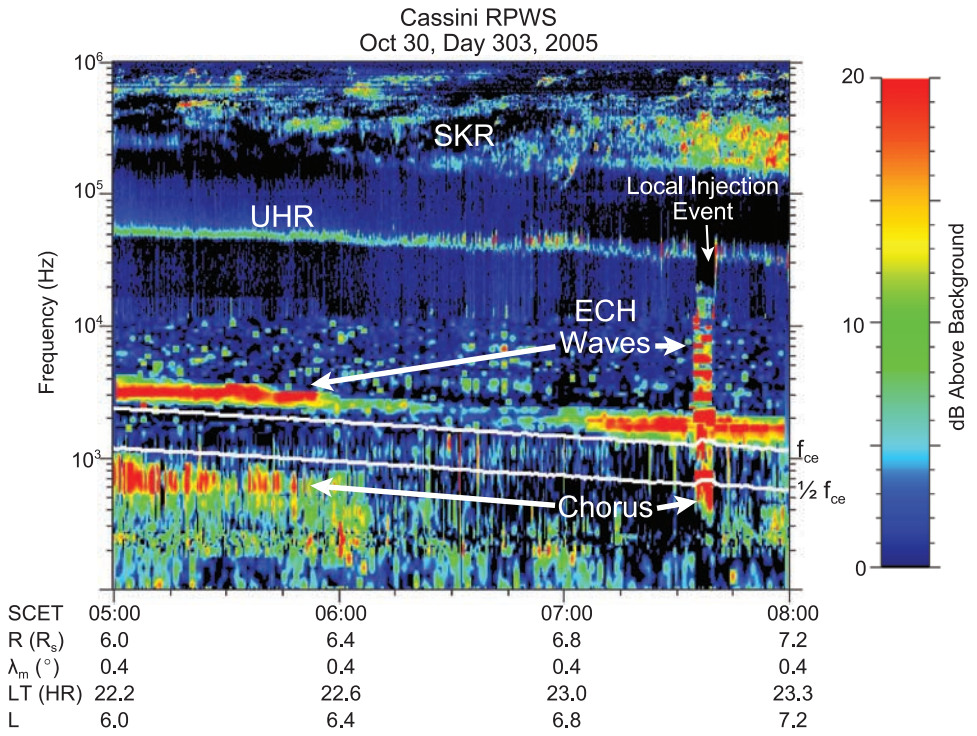

Figure 4. A time-frequency spectrogram from Orbit 17 of the electric field survey data which shows the wide range of emissions that are detected by RPWS in Saturn's magnetosphere. "Magnetospheric" chorus is observed below 1/2 f_{ce} from 0500 SCET to about 0600 SCET (this is a continuation of the chorus shown in Figure 3d). From about 0735 to 0740 SCET, the characteristics of the plasma waves indicate the presence of a local injection event.

[15] A second type of chorus detected by Cassini at Saturn is associated with local electron injections. These inwardly injected flux tubes of low-density, warmer (100s to 1000s eV) electrons are often detected in Saturn's inner magnetosphere [*Burch et al.*, 2005; *Hill et al.*, 2005; *Mauk et al.*, 2005; *Paranicas et al.*, 2007; *Rymer et al.*, 2007, 2008] and are important in balancing the outward flow of the higher-density, cool (<100 eV) electrons in a rotationally dominated magnetosphere. Figure 4 is a time-frequency spectrogram from Orbit 17 of the electric field survey data which shows the wide range of emissions that are detected by RPWS in Saturn's magnetosphere. Saturn kilometric radio emission (SKR) is detected almost continuously in this period above about 100 kHz. The upper hybrid resonance (UHR) emission is seen throughout most of this period, starting at about 50 kHz at the 0500 SCET and dropping to about 30 kHz at 0800 SCET. From the frequency of this emission, and the magnetic field value provided by the Magnetometer instrument, the local electron plasma density can be determined (see *Persoon et al.* [2005, 2006a, 2006b] for density measurement results in Saturn's inner magnetosphere using this technique). Electrostatic electron cyclotron harmonic (ECH) waves, also called n+1/2 harmonic waves, are detected just above f_{ce} during most of this interval. "Magnetospheric" chorus is observed below 1/2 f_{ce} from 0500 SCET to about 0600 SCET (this is a continuation of the chorus shown in Figure 3d).

[16] From about 0735 to 0740 SCET, the characteristics of many of the plasma waves change. First, the UHR either disappears, or more likely drops in frequency (corresponding to a drop in density of the background plasma). Second, there occurs an intensification of the ECH waves and the appearance of additional harmonics. Third, there is an appearance of strong chorus emission at about 1/2 f_{ce}. The local magnetic field also increased at this time, represented by the increase in f_{ce} and 1/2 f_{ce}. The characteristics of the ECH and chorus emissions of this event can be more easily seen in the high-resolution WBR time-frequency spectrograms shown in Figure 5. The top panel shows the ECH waves, and the appearance of the more complicated ECH harmonic structure during the injection event. The bottom panel focuses on the chorus emission that appears near 1/2 f_{ce} during the event. These changes in the plasma wave emissions are evidence for the occurrence of a local injection event, and this hypothesis has been confirmed by *Rymer et al.* [2008] from the Cassini Plasma Spectrometer (CAPS) electron data for this event. Their initial analysis of the CAPS data for this event finds that inside the injection, the low-energy (<100 eV) electrons flux is reduced, while the high-energy component (>1 keV) is enhanced. The higher-energy component forms pancake-like distributions while the lower-energy electrons are more field aligned [*Rymer et al.*, 2008, Figure 5]. *Menietti et al.* [2008a] has examined this specific event and modeled the measured electron plasma distributions to conduct linear dispersion analysis of the plasma wave modes, especially for the ECH waves. They find that a narrow loss cone for the lower-energy electrons distribution can drive growth of oblique ECH waves similar to those that are observed. They also found that the higher-energy pancake-like distribution with

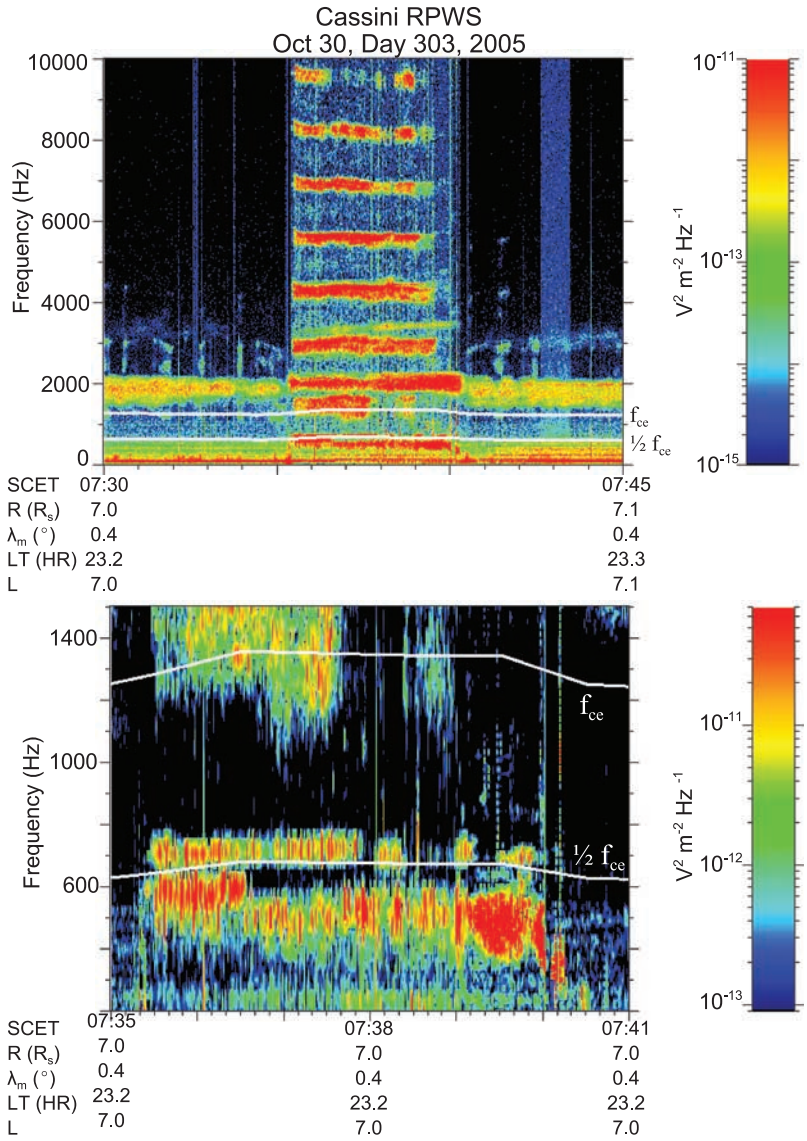

Figure 5. High-rate WBR time-frequency spectrograms from Orbit 17: (top) the structure of ECH emissions and (bottom) the chorus emission detected during the injection event. As can be seen, the "injection event" chorus has a gap at 1/2 f_{ce} and fine structure with a smaller time scale than most of the "magnetospheric" chorus events shown in Figure 3.

a temperature anisotropy can drive whistler mode waves, although at a lower frequency than the chorus observed for this event.

[17] An examination of the chorus shown in the bottom panel of Figure 5 shows that this chorus has different characteristics from the "magnetospheric" chorus examples shown in Figure 3. The most noticeable difference is that the chorus occurs in two bands, separated by a gap at about 1/2 f_{ce}. This appearance is very similar to chorus detected at the Earth, and the only detection of chorus at Saturn with frequencies greater than 1/2 f_{ce} is during local injection events. The chorus emissions also appear to be more bursty than the examples shown on Figure 3, are only detected for a few minutes, and are not observed immediately outside of the injection event. Figure 6 shows two other examples of high-resolution WBR time-frequency spectrograms obtained during two injection events from orbit 4. Both show the gap at 1/2 f_{ce} and both show a series of rising tones in the lower band of chorus, very similar in appearance to chorus at the Earth. These examples are very typical of the "injection event" chorus when it is detected at Saturn.

[18] A survey of all the RPWS WFR data has been completed for the first 45 orbits (including Saturn Orbit Insertion) of Saturn, and the periods for which chorus (both "typical" and "injection event" chorus) is present have been determined. The wave normal analysis has been performed on each chorus event, and the propagation characteristics of the chorus at Saturn with respect to the Saturn magnetic field are shown in Figure 7. Green on Figure 7 refers to wave propagation anti-parallel to the magnetic field (northward propagation away from the magnetic equator), red refers to parallel propagation (southward propagation), and blue shows mixed propagation directions. As can be seen, the chorus at Saturn always

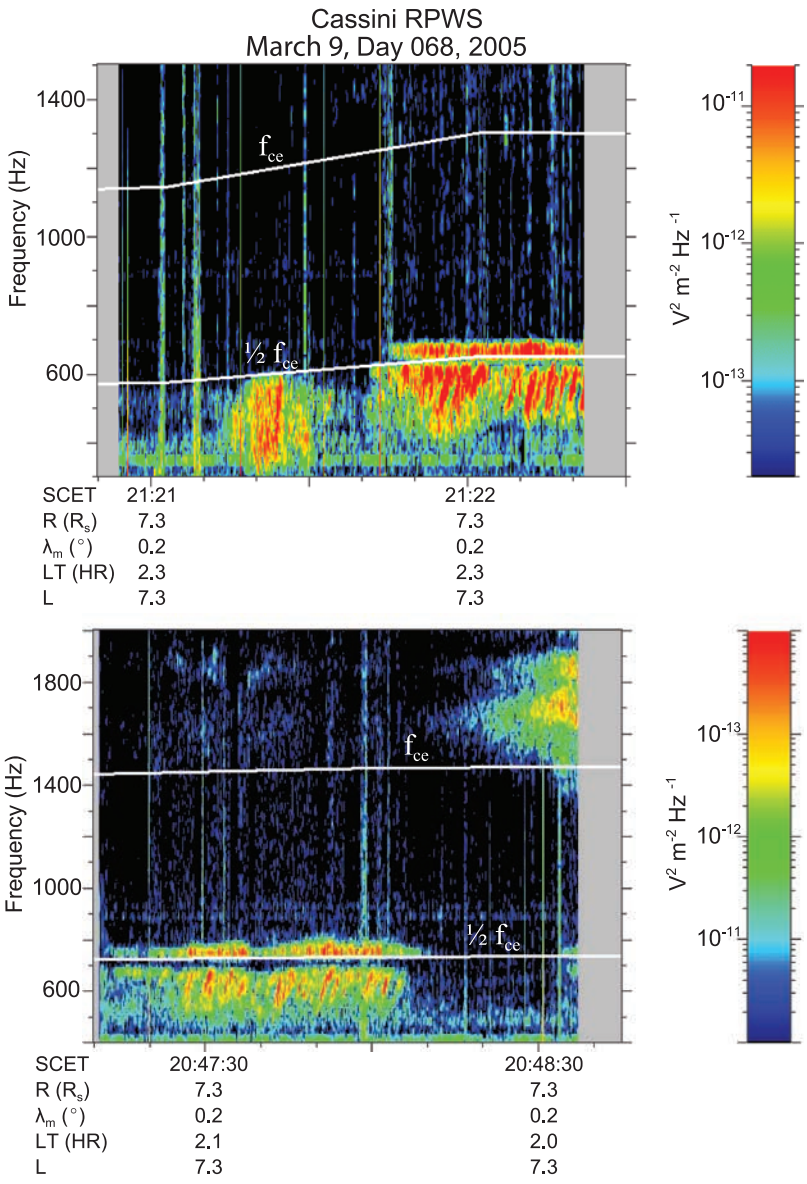

Figure 6. Two high-resolution WBR time-frequency spectrograms obtained during two injection events from orbit 4. Both examples show the gap at 1/2 f_{ce}, and both show a series of rising tones in the lower band of chorus, very similar in appearance to chorus at the Earth. These two examples are very typical of the "injection event" chorus when it is detected at Saturn.

propagates away from the magnetic equator except for regions very near the equator, which is very similar to the results of *LeDocq et al.* [1998] for the Earth. It should be noted that the magnetic equator (y axis = 0) shown in Figure 7 is determined from a model magnetic field of Saturn. A closer examination of the results very near the model magnetic equator shows a few cases of purely southward propagating chorus (not mixed) observed up to 0.8° north of the predicted magnetic equator, but no purely northward propagating chorus has been detected south of the predicted magnetic equator. This discrepancy could be explained by a slight shift northward of the expected magnetic equator location, which has been suggested by MAG measurements of the plasma sheet [*Arridge et al.*, 2008; K. K. Khurana et al., Sources of rotational signals in Saturn's magnetosphere, submitted to *Journal of Geophysical Research*, 2008].

[19] The relationships between the detection of chorus and the various orbital parameters of the Cassini spacecraft have also been examined for the first 45 orbits. Figure 8 shows the occurrence of the chorus (solid dots) with respect to L shell versus local time (bottom panel) and latitude (top panels) for the "magnetospheric" chorus (two left panels) and the "injection event" chorus (two right panels). The dashed lines in the two left panels are the trajectory of Cassini during the first 45 orbits to show the orbital coverage for this period. As can be seen from the two left panels, there is no obvious correlation between the occurrence of the "magnetospheric" chorus and local time or latitude. From the bottom right panel, no local time dependence for the occurrence of "injection event"

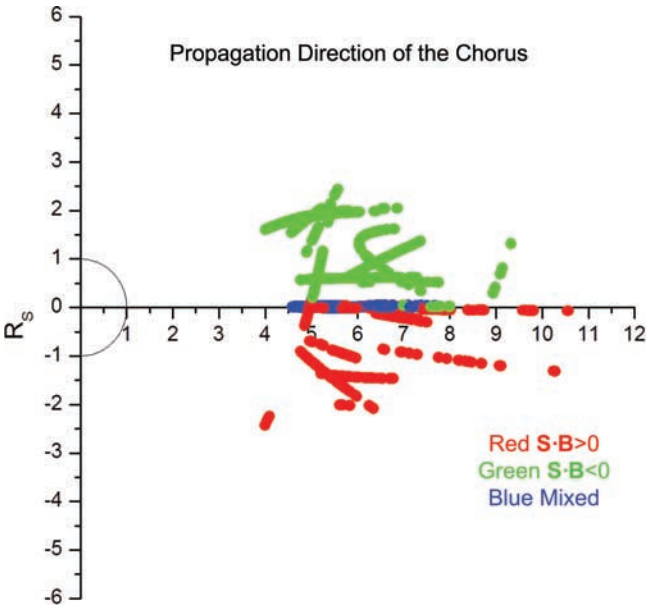

Figure 7. The propagation direction of the chorus emission detected at Saturn with respect to the magnetic field shown on a magnetic meridian plot. The chorus emission at Saturn usually propagates away from the magnetic equator. Very near the equator, a mixture of both upward and downward propagation is observed.

chorus can be seen. However, it appears that "injection event" chorus is more likely to be observed near the magnetic equator. Both the "magnetospheric" and "injection event" chorus primarily occurs between L shells of about 4.7 to 8. "Magnetospheric" chorus also appears at greater L shells (8 to about 10.5), but only around local noon and near the magnetic equator. An examination of these chorus events at larger L shells shows that the occurrence of the chorus is often correlated with enhancements in the UHR intensity and broadening of the bandwidth of the UHR emission. An example of this correlation from orbit 22 is shown in Figure 9. The broadening and especially the intensification of the UHR band suggests an instability as opposed to a thermal emission is responsible for the UHR enhancements. The possibility of similar electron distributions driving both the UHR band and the chorus will be investigated in more detail in future work. The possible correlation between the occurrence of the chorus and the new SLS2 longitude [*Kurth et al.*, 2007] system was also examined for the first 23 orbits and no correlation was found.

[20] The amplitude of the chorus emissions is important in understanding the possible wave-particle interactions. For example, at the Earth typical chorus amplitudes are usually around 0.01 to 0.1 nT, and may reach 300 nT (or 30 mV/m) during disturbed periods [*Santolik et al.*, 2006]. *Cattell et al.* [2008] using recent results from the Stereo spacecraft have reported even larger amplitude electric field signals (240 mV/m) associated with high time resolution measurements in the Van Allen radiation belts, and suggest that strong nonlinear wave-particle processes may be more important than earlier thought. At Jupiter, *Coroniti et al.* [1980, 1984] using Voyager observations reported chorus amplitudes of about 0.26 mV/m (10 pT assuming parallel propagation). Similar amplitudes of about 0.1 mV/m and 3 pT have recently been reported using the Galileo observations [*Horne et al.*, 2008; *Menietti et al.*, 2008b]. At Saturn, *Scarf et al.* [1983] reported average chorus electric field amplitudes at 1 kHz of about 1.8×10^{-3} mV/m(Hz)$^{1/2}$, and estimated (Voyager did not have a search coil magnetometer) a magnetic field wave amplitude of 0.15 pT/(Hz)$^{1/2}$ from the calculated index of refraction assuming parallel propagation. Using the bandwidth of 133 Hz for the 1 kHz Voyager channel, this gives an electric field amplitude of about 0.02 mV/m and magnetic field amplitude of 2 pT. Using these values and the plasma conditions measured by Voyager during the period chorus was detected, *Scarf et al.* [1983, 1984] found the waves too weak to play a significant role in pitch angle scattering of the electrons.

[21] The Cassini spacecraft, with the simultaneous measurements of electric and magnetic field components of the waves with the WFR, and high time and frequency resolution measurements with the WBR, allows a more detailed examination of the chorus wave amplitude at Saturn than was possible with Voyager. The top part of Table 1 shows the measured electric and magnetic field wave amplitudes of the "magnetospheric" chorus examples from each panel of Figure 3, and the bottom part of Table 1 shows electric and magnetic field wave amplitudes for the "injection event" chorus examples shown in Figures 5 and 6. The first column shows the time of the measurement in spacecraft event time (SCET) and the second column shows the receiver that supplied the measurement. The time shown for the WFR data is the start of the waveform capture, and the amplitudes are obtained from FFTs of each 2048 sample waveform (about 0.29 s long). All of the WFR data that were obtained in the periods shown in Figures 3 (except for Figure 3d), 5 and 6 are included in Table 1. The times chosen for the WBR measurements were periods where the chorus emission exhibited the narrowband-tone fine structure or the period of the largest wave amplitudes that occurred during the spectrograms shown in Figures 3, 5, and 6. The columns 3, 4, and 5 show the frequency corresponding to the peak amplitude of the chorus, the electric field wave amplitude, and the magnetic field wave amplitude. The last column shows the corresponding figure that contains this time period. For the "injection event" chorus, this column also shows if the measurement was for the chorus observed above or below 1/2 f_{ce}.

[22] As can be seen, the amplitudes of the chorus emissions at Saturn vary by more than an order of magnitude. The WFR electric field results ranged from about 2×10^{-6} V m^{-1} Hz$^{-1/2}$ to 2×10^{-5} V m^{-1} Hz$^{-1/2}$ and the magnetic field results ranged from about 1×10^{-4} nT Hz$^{-1/2}$ to 5×10^{-3} nT Hz$^{-1/2}$. The peak electric fields amplitudes measured by the WBR ranged from about 2×10^{-6} V m^{-1} Hz$^{-1/2}$ to 1×10^{-4} V m^{-1} Hz$^{-1/2}$. Assuming a bandwidth of the chorus of 50 Hz (the fine structure ranges from a few tens of Hz to hundreds of Hz), the electric field amplitudes range from about 0.01 mV/m to about 1 mV/m and the magnetic field amplitudes range from about 0.5 pT to about 35 pT. The lower range of amplitudes measured by Cassini are similar to the Voyager results of 1.76×10^{-6} V m^{-1} Hz$^{-1/2}$ (0.02 mV/m) and 1.54×10^{-4} nT Hz$^{-1/2}$ (2 pT) reported by *Scarf et al.* [1983, 1984]. However, the upper

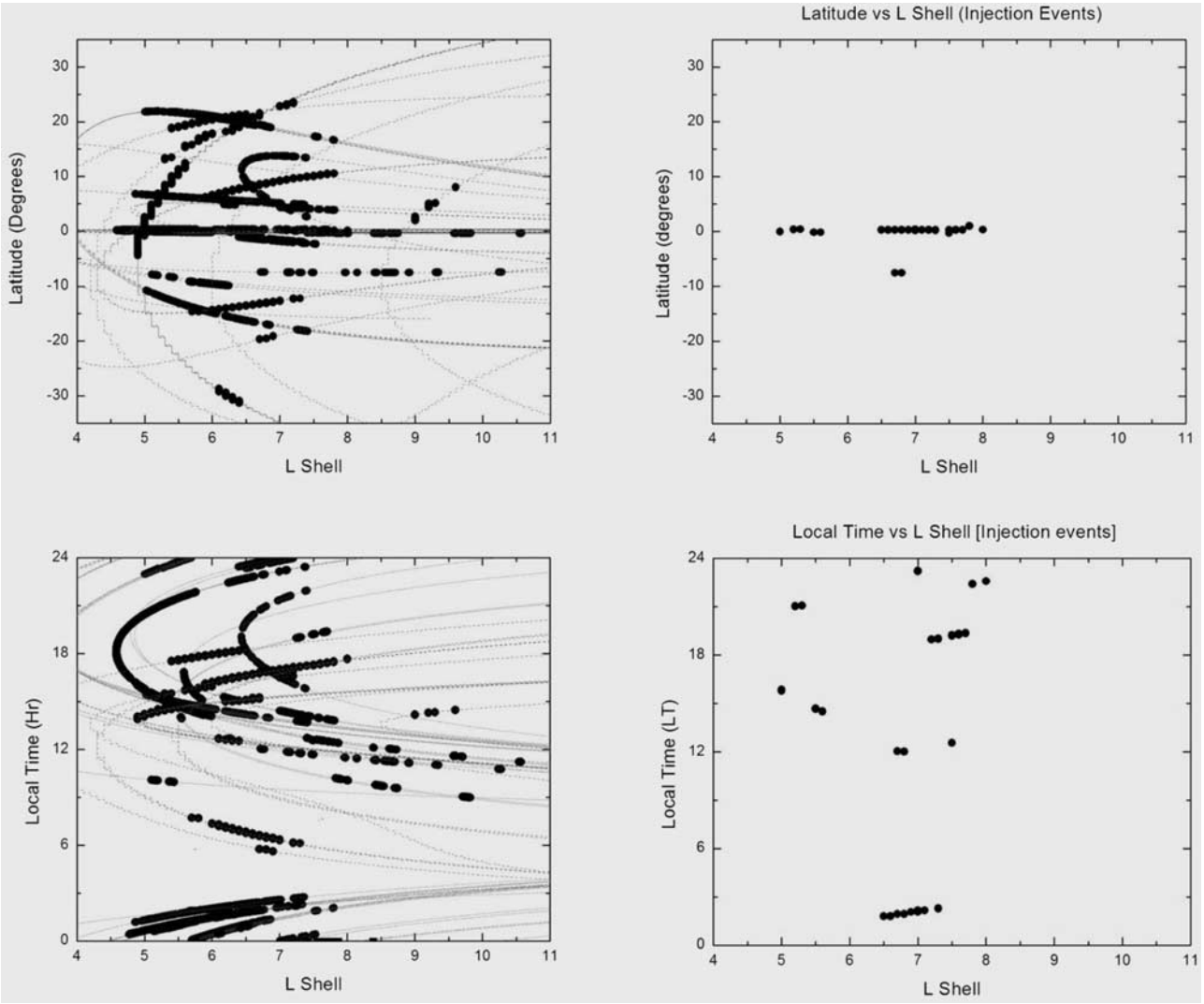

Figure 8. The position of Cassini during the periods that the "magnetospheric" (left panels) and "injection event" (right panels) chorus is detected. The top panels show latitude versus L shell, and the bottom panels show local time (LT) versus L shell.

range of the Cassini results are at least an order of magnitude higher than the Voyager results, suggesting that the waves-particle interaction may be more important during these periods.

[23] Whistler mode waves propagating parallel to the magnetic field, assuming the cold plasma approximation, will resonate with electrons of energy

$$E(\text{res}) \approx \tfrac{1}{2}mc^2(f_{ce}-f)^2/(nf)^2, \quad (1)$$

where m is the mass of the electron, c is the speed of light, f is the frequency of the whistler wave, and n is the index of refraction given by

$$n^2 = 1 + f_{pe}^2/\left(ff_{ce}-f^2\right), \quad (2)$$

where f_{pe} is the electron plasma frequency [*Scarf et al.*, 1984]. Table 2 shows the electron plasma frequency, electron cyclotron frequency, frequency of the chorus, the calculated index of refraction from equation (2), and the estimated resonant energy calculated from equation (1) for the chorus detected on October 30, 2005 (Figures 3d, 4 and 5). This period was chosen because both "magnetospheric" and "injection event" chorus were detected during this orbit, and the chorus was observed near the magnetic equator. The resonance energies for this example ranged from a few hundred eV to slightly less than 1 keV, with similar values calculated both for the "magnetospheric" chorus and for the "injection event" chorus. An initial examination of the CAPS electron data during this event show some electrons with similar energies, but a more detailed comparison will be presented in a future work to determine the importance at Saturn of chorus and other whistler mode emissions in wave-particle interactions.

5. Conclusions

[24] Whistler mode chorus emissions are observed by the RPWS instrument during most orbits of Saturn, and are

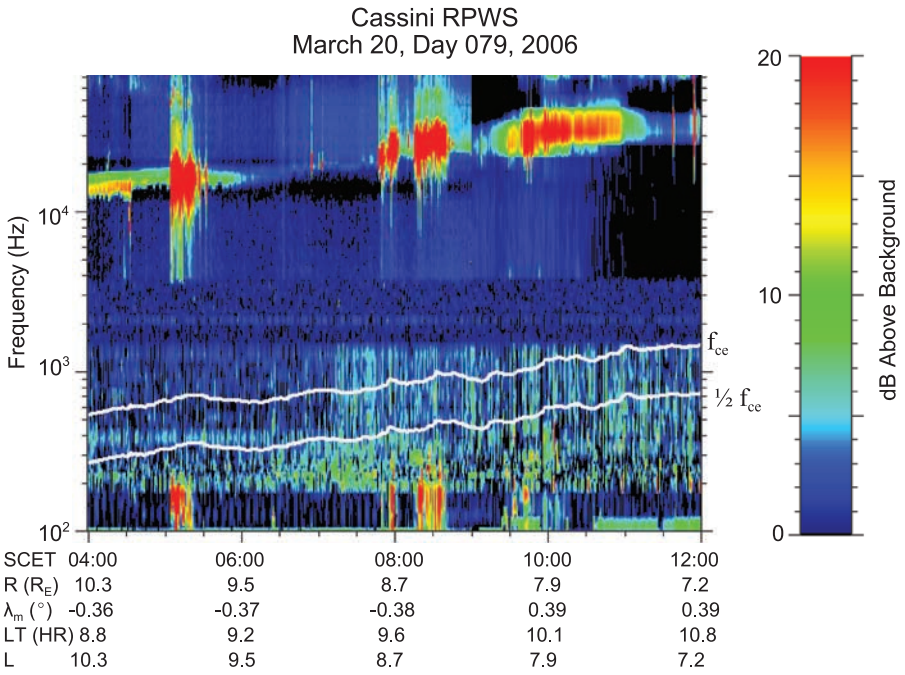

Figure 9. A time-frequency spectrogram from Orbit 22 showing the correlation between the enhanced UHR and the occurrence of chorus emission at higher *L* shells.

detected in two different regions. The most common observations (''magnetospheric'' chorus) are of emissions that are usually detected for many hours and are propagating away from Saturn's magnetic equator. This ''magnetospheric'' chorus is only observed below half the electron cyclotron frequency and occurs primarily from *L* shells of about 5 to 8, and shows no correlation with Saturn magnetic latitude, longitude, or local time. ''Magnetospheric'' chorus detected at larger *L* shells (between *L* of 8 to 10) is usually confined to lower latitudes and occurs at local times near noon. High-resolution measurements show that the fine structure that is observed usually consists of rising tones, but with larger time scales (many seconds to minutes) than typically observed at the Earth (<1 s). The second region of chorus detected at Saturn is in association with local plasma injections (''injection event'' chorus). For many plasma injection events, chorus emissions are detected both above and below half the electron cyclotron frequency, with a gap in the emission at half the cyclotron frequency. This chorus is usually only detected for a few minutes, is not observed outside of the injection event, contains fine structure (usually a series of rising tones) at a much smaller time scale (less than a second to a few seconds) than the ''magnetospheric'' chorus, and appears similar to chorus detected at the Earth. These differences and similarities of the fine structure of chorus detected in different regions at Saturn compared to the chorus detected at the Earth may help in understanding the source of this fine structure. An initial

Table 1. Measured Electric and Magnetic Field Wave Amplitudes

Time (SCET)	Receiver	Freq. (Hz)	Electric (V/m(Hz)$^{1/2}$)	Magnetic (nT/(Hz)$^{1/2}$)	Notes
			''Magnetospheric'' Chorus		
2005-05-21T10:29:59.000	WFR	580	2.2×10^{-6}	2.2×10^{-4}	Figure 3a
2004-10-28T09:46:33.524	WFR	400	8.4×10^{-6}	1.4×10^{-3}	Figure 3b
2004-10-28T09:47:25.400	WBR	400	1.4×10^{-5}	-	Figure 3b tones
2004-10-28T09:47:13.600	WBR	300	1.4×10^{-5}	-	Figure 3b tones
2004-10-28T09:38:45.600	WBR	500	6.3×10^{-6}	-	Figure 3c tones
2005-10-30T02:12:29.799	WFR	1600	2.4×10^{-6}	3.2×10^{-4}	Figure 3d
2005-10-30T03:43:09.764	WFR	800	2.6×10^{-6}	4.5×10^{-4}	Figure 3d
			''Injection Event'' Chorus		
2005-10-30T07:37:49.675	WFR	550	5.5×10^{-5}	7.1×10^{-4}	Figure 5b
2005-10-30T07:37:49.675	WFR	725	1.5×10^{-5}	1.7×10^{-4}	Figure 5b
2005-10-30T07:37:42.840	WBR	550	1.0×10^{-4}	-	Figure 5b below 1/2 f_{ce}
2005-10-30T07:37:26.760	WBR	725	2.5×10^{-5}	-	Figure 5b above 1/2 f_{ce}
2005-03-09T21:21:19.164	WFR	450	4.5×10^{-6}	7.8×10^{-4}	Figure 6a
2005-03-09T21:22:11.672	WBR	540	2.0×10^{-5}	-	Figure 6a below 1/2 f_{ce}
2005-03-09T21:22:11.800	WBR	680	1.7×10^{-5}	-	Figure 6a above 1/2 f_{ce}
2005-03-09T20:47:34.560	WBR	650	1.0×10^{-5}	-	Figure 6b below 1/2 f_{ce}
2005-03-09T20:49:36.800	WBR	750	1.7×10^{-5}	-	Figure 6b above 1/2 f_{ce}
2005-03-09T20:49:19.177	WFR	650	2.5×10^{-5}	4.5×10^{-3}	after Figure 6b
2005-03-09T20:49:19.177	WFR	750	3.2×10^{-5}	5.0×10^{-3}	after Figure 6b

Table 2. Estimated Resonant Energies

Time (SCET)	f_{pe} (kHz)	f_{ce} (kHz)	f (kHz)	n	E_{res} (keV)
"Magnetospheric" Chorus: 2005-10-30					
2005-10-30T02:12:29.799	68.0	4.2	1.6	33	0.61
2005-10-30T03:43:09.764	60.0	3.0	0.8	45	0.94
"Injection Event" Chorus: 2005-10-30					
2005-10-30T07:37:49.675	19.0	1.35	550	29	0.66
2005-10-30T07:37:49.675	19.0	1.35	725	28	0.24

examination of the peak wave amplitudes of the chorus emissions at Saturn finds amplitudes much smaller than the peak amplitudes that have been reported at the Earth, but larger by at least an order of magnitude than the amplitudes detected by Voyager. The detection of these larger amplitudes suggests that chorus may be responsible for some pitch angle diffusion at Saturn. The importance of these waves in wave-particle interaction at Saturn will be presented in a future work.

[25] **Acknowledgments.** The research at The University of Iowa is supported by the National Aeronautics and Space Administration through contract 1279973 with the Jet Propulsion Laboratory. The authors would also like to acknowledge the Cassini data analysis program which will support some of the future work on plasma waves at Saturn discussed in this paper.

[26] Amitava Bhattacharjee thanks Bruce Goldstein and another reviewer for their assistance in evaluating this paper.

References

Allcock, G. M. (1957), A study of the audio-frequency radio phenomenon known as ''dawn chorus'', *Aust. J. Phys.*, *10*, 286.

Anderson, R. R., and K. Maeda (1977), VLF emissions associated with enhanced magnetospheric electrons, *J. Geophys. Res.*, *82*, 135–146, doi:10.1029/JA082i001p00135.

Arridge, C. S., K. K. Khurana, C. T. Russell, D. J. Southwood, N. Achilleos, M. K. Dougherty, A. J. Coates, and H. K. Leinweber (2008), Warping of Saturn's magnetospheric and magnetotail current sheets, *J. Geophys. Res.*, *113*, A08217, doi:10.1029/2007JA012963.

Bortnik, J., and R. M. Thorne (2007), The dual role of ELF/VLF chorus waves in the acceleration and precipitation of radiation belt electrons, *J. Atmos. Sol. Terr. Phys.*, *69*, 378–386, doi:10.1016/j.jastp.2006.05.030.

Breneman, A., C. A. Kletzing, J. Chum, O. Santolik, D. A. Gurnett, and J. S. Pickett (2007), Multispacecraft observations of chorus dispersion and source location, *J. Geophys. Res.*, *112*, A05221, doi:10.1029/2006JA012058.

Burch, J. L., J. Goldstein, T. W. Hill, D. T. Young, F. J. Crary, A. J. Coates, N. Andre, W. S. Kurth, and E. C. Sittler Jr. (2005), Properties of local plasma injections in Saturn's magnetosphere, *Geophys. Res. Lett.*, *32*, L14S02, doi:10.1029/2005GL022611.

Burtis, W. J., and R. A. Helliwell (1969), Banded chorus—A new type of VLF radiation observed in the magnetosphere by OGO 1 and OGO 3, *J. Geophys. Res.*, *74*, 3002–3010, doi:10.1029/JA074i011p03002.

Burton, R. K. (1976), Critical electron pitch angle anisotropy necessary for chorus generation, *J. Geophys. Res.*, *81*, 4779–4781, doi:10.1029/JA081i025p04779.

Burton, R., and R. E. Holzer (1974), The origin and propagation of chorus in the outer magnetosphere, *J. Geophys. Res.*, *79*, 1014–1023, doi:10.1029/JA079i007p01014.

Cattell, C., et al. (2008), Discovery of very large amplitude whistler-mode waves in Earth's radiation belts, *Geophys. Res. Lett.*, *35*, L01105, doi:10.1029/2007GL032009.

Chum, J., O. Santolik, A. W. Breneman, C. A. Kletzing, D. A. Gurnett, and J. S. Pickett (2007), Chorus source properties that produce time shifts and frequency range differences observed on different spacecraft, *J. Geophys. Res.*, *112*, A06206, doi:10.1029/2006JA012061.

Cornilleau-Wehrlin, N., R. Gendrin, F. Lefeuvre, M. Parrot, R. Grard, D. Jones, A. Bahnsen, E. Ungstrup, and W. Gibbons (1978), VLF electromagnetic waves observed onboard GEOS-1, *Space Sci. Rev.*, *22*, 371–382.

Coroniti, F. V., F. L. Scarf, C. F. Kennel, W. S. Kurth, and D. A. Gurnett (1980), Detection of Jovian whistler mode chorus: Implications for the Io torus aurora, *Geophys. Res. Lett.*, *7*, 45–48, doi:10.1029/GL007i001p00045.

Coroniti, F. V., F. L. Scarf, C. F. Kennel, and W. S. Kurth (1984), Analysis of chorus emissions at Jupiter, *J. Geophys. Res.*, *89*, 3801–3820, doi:10.1029/JA089iA06p03801.

Curtis, S. A. (1978), A theory for chorus generation by energetic electrons during substorms, *J. Geophys. Res.*, *83*, 3841–3848, doi:10.1029/JA083iA08p03841.

Dougherty, M. K., et al. (2004), The Cassini magnetic field investigation, *Space Sci. Rev.*, *114*, 331–383, doi:10.1007/s11214-004-1432-2.

Dunckel, N., and R. A. Helliwell (1969), Whistler mode emissions on the OGO-1 satellite, *J. Geophys. Res.*, *74*, 6371–6385, doi:10.1029/JA074i026p06371.

Goldstein, B. E., and B. T. Tsurutani (1984), Wave normal directions of chorus near the equatorial source region, *J. Geophys. Res.*, *89*, 2789–2810, doi:10.1029/JA089iA05p02789.

Gurnett, D. A., and B. J. O'Brien (1964), High-latitude geophysical studies with satellite Injun 3: 5. Very-low-frequency electromagnetic radiation, *J. Geophys. Res.*, *69*, 65–89, doi:10.1029/JZ069i001p00065.

Gurnett, D. A., W. S. Kurth, and F. L. Scarf (1981), Plasma waves near Saturn: Initial results from Voyager 1, *Science*, *212*, 235–239, doi:10.1126/science.212.4491.235.

Gurnett, D. A., et al. (2004), The Cassini radio and plasma wave science investigation, *Space Sci. Rev.*, *114*, 395–463, doi:10.1007/s11214-004-1434-0.

Hayakawa, M., Y. Yamanaka, M. Parrot, and F. Lefeuvre (1984), The wave normals of magnetospheric chorus emissions observed on board GEOS 2, *J. Geophys. Res.*, *89*, 2811–2821, doi:10.1029/JA089iA05p02811.

Hayakawa, M., K. Hattori, S. Shimakura, M. Parrot, and F. Lefeuvre (1990), Direction finding of chorus emissions in the outer magnetosphere and their generation and propagation, *Planet. Space Sci.*, *38*, 135–143, doi:10.1016/0032-0633(90)90012-F.

Helliwell, R. A. (1969), Low-frequency waves in the magnetosphere, *Rev. Geophys.*, *7*, 281–303, doi:10.1029/RG007i001p00281.

Hill, T. W., A. M. Rymer, J. L. Burch, F. J. Crary, D. T. Young, M. F. Thomsen, D. Delapp, N. Andre, A. J. Coates, and G. R. Lewis (2005), Evidence for rotationally driven plasma transport in Saturn's magnetosphere, *Geophys. Res. Lett.*, *32*, L14S10, doi:10.1029/2005GL022620.

Horne, R. B., S. A. Glauert, and R. M. Thorne (2003), Resonant diffusion of radiation belt electrons by whistler-mode chorus, *Geophys. Res. Lett.*, *30*(9), 1493, doi:10.1029/2003GL016963.

Horne, R. B., R. M. Thorne, S. A. Glauert, J. M. Albert, N. P. Meredith, and R. R. Anderson (2005), Timescale for radiation belt electron acceleration by whistler mode chorus waves, *J. Geophys. Res.*, *110*, A03225, doi:10.1029/2004JA010811.

Horne, R. B., R. M. Thorne, S. A. Glauert, J. D. Menietti, Y. Y. Shprits, and D. A. Gurnett (2008), Gyro-resonant electron acceleration at Jupiter, *Nature Phys.*, *4*, 301–304, doi:10.1038/nphys897.

Hospodarsky, G. B., T. F. Averkamp, W. S. Kurth, D. A. Gurnett, M. Dougherty, U. Inan, and T. Wood (2001), Wave normal and Poynting vector calculations using the Cassini radio and plasma wave instrument, *J. Geophys. Res.*, *106*, 30,253–30,269, doi:10.1029/2001JA900114.

Inan, U. S., Y. T. Chiu, and G. T. Davidson (1992), Whistler-mode chorus and morningside aurorae, *Geophys. Res. Lett.*, *19*, 653–656, doi:10.1029/92GL00402.

Inan, U. S., M. Platino, T. F. Bell, D. A. Gurnett, and J. S. Pickett (2004), Cluster measurements of rapidly moving sources of ELF/VLF chorus, *J. Geophys. Res.*, *109*, A05214, doi:10.1029/2003JA010289.

Isenberg, P. A., H. C. Koons, and J. F. Fennell (1982), Simultaneous observations of energetic electrons and dawnside chorus in geosynchronous orbit, *J. Geophys. Res.*, *87*, 1495–1503, doi:10.1029/JA087iA03p01495.

Katoh, Y., and Y. Omura (2007), Relativistic particle acceleration in the process of whistler-mode chorus wave generation, *Geophys. Res. Lett.*, *34*, L13102, doi:10.1029/2007GL029758.

Kennel, C. F., and H. E. Petschek (1966), Limit on stably trapped particle fluxes, *J. Geophys. Res.*, *71*, 1–28.

Kurth, W. S., and D. A. Gurnett (1991), Plasma waves in planetary magnetospheres, *J. Geophys. Res.*, *96*, 18,977–18,991.

Kurth, W. S., A. Lecacheux, T. F. Averkamp, J. B. Groene, and D. A. Gurnett (2007), A Saturnian longitude system based on a variable kilometric radiation period, *Geophys. Res. Lett.*, *34*, L02201, doi:10.1029/2006GL028336.

Lauben, D. S., U. S. Inan, T. F. Bell, D. L. Kirchner, G. B. Hospodarsky, and J. S. Pickett (1998), VLF chorus emissions observed by Polar during the January 10, 1997, magnetic cloud, *Geophys. Res. Lett.*, *25*, 2995–2998, doi:10.1029/98GL01425.

Lauben, D. S., U. S. Inan, T. F. Bell, and D. A. Gurnett (2002), Source characteristics of ELF/VLF chorus, *J. Geophys. Res.*, *107*(A12), 1429, doi:10.1029/2000JA003019.

LeDocq, M. J. (1998), Wave normal and Poynting flux directions of magnetospheric plasma waves, Ph.D. thesis, 178 pp., Univ. of Iowa, Iowa City.

LeDocq, M. J., D. A. Gurnett, and G. B. Hospodarsky (1998), Chorus source location from VLF Poynting flux measurements with the Polar spacecraft, *Geophys. Res. Lett.*, *25*, 4063–4066, doi:10.1029/1998GL900071.

Mauk, B. H., et al. (2005), Energetic particle injections in Saturn's magnetosphere, *Geophys. Res. Lett.*, *32*, L14S05, doi:10.1029/2005GL022485.

Means, J. D. (1972), Use of the three-dimensional covariance matrix in analyzing the polarization properties of plane waves, *J. Geophys. Res.*, *77*, 5551–5559, doi:10.1029/JA077i028p05551.

Menietti, J. D., O. Santolik, A. M. Rymer, G. B. Hospodarsky, A. M. Persoon, D. A. Gurnett, A. J. Coates, and D. T. Young (2008a), Analysis of plasma waves observed within local plasma injections seen in Saturn's magnetosphere, *J. Geophys. Res.*, *113*, A05213, doi:10.1029/2007JA012856.

Menietti, J. D., D. A. Gurnett, G. B. Hospodarsky, R. Horne, and J. B. Groene (2008b), A survey of Galileo plasma wave instrument observations of Jovian whistler-mode chorus, *Ann. Geophys.*, *26*, 1819–1828.

Meredith, N. P., R. B. Horne, and R. R. Anderson (2001), Substorm dependence of chorus amplitides: Implications for the acceleration of electrons to relativistic energies, *J. Geophys. Res.*, *106*, 13,165–13,178, doi:10.1029/2000JA900156.

Nagano, I., S. Yagitani, H. Kojima, and H. Matsumoto (1996), Analysis of wave normal and Poynting vectors of chorus emissions observed by Geotail, *J. Geomagn. Geoelectr.*, *48*, 299–307.

Omura, Y., and D. Summers (2006), Dynamics of high-energy electrons interacting with whistler mode chorus emissions in the magnetosphere, *J. Geophys. Res.*, *111*, A09222, doi:10.1029/2006JA011600.

Omura, Y., Y. Katoh, and D. Summers (2008), Theryand simulation of the generation of whistler-mode chorus, *J. Geophys. Res.*, *113*, A04223, doi:10.1029/2007JA012622.

Paranicas, C., D. G. Mitchell, E. C. Roelof, B. H. Mauk, S. M. Krimigis, P. C. Brandt, M. Dusterer, F. S. Turner, J. Vandegriff, and N. Krupp (2007), Energetic electrons injected into Saturn's neutral gas cloud, *Geophys. Res. Lett.*, *34*, L02109, doi:10.1029/2006GL028676.

Parrot, M., O. Santolik, N. Cornilleau-Wehrlin, M. Maksimovic, and C. C. Harvey (2003), Source location of chorus emissions observed by Cluster, *Ann. Geophys.*, *21*, 473–480.

Persoon, A. M., D. A. Gurnett, W. S. Kurth, G. B. Hospodarsky, J. B. Groene, P. Canu, and M. K. Dougherty (2005), Equatorial electron density measurements in Saturn's inner magnetosphere, *Geophys. Res. Lett.*, *32*, L23105, doi:10.1029/2005GL024294.

Persoon, A. M., D. A. Gurnett, W. S. Kurth, G. B. Hospodarsky, J. B. Groene, P. Canu, and M. K. Dougherty (2006a), An electron density model for Saturn's inner magnetosphere, in *Planetary Radio Emissions VI*, edited by H. O. Rucker, W. S. Kurth, and G. Mann, pp. 81–91, Austrian Acad. of Sci. Press, Vienna.

Persoon, A. M., D. A. Gurnett, W. S. Kurth, and J. B. Groene (2006b), A simple scale height model of the electron density in Saturn's plasma disk, *Geophys. Res. Lett.*, *33*, L18106, doi:10.1029/2006GL027090.

Rymer, A. M., et al. (2007), Electron sources in Saturn's magnetosphere, *J. Geophys. Res.*, *112*, A02201, doi:10.1029/2006JA012017.

Rymer, A. M., B. H. Mauk, T. W. Hill, C. Paranicas, D. G. Mitchell, A. J. Coates, and D. T. Young (2008), Electron circulation in Saturn's magnetosphere, *J. Geophys. Res.*, *113*, A01201, doi:10.1029/2007JA012589.

Santolik, O., and D. A. Gurnett (2003), Transverse dimensions of chorus in the source region, *Geophys. Res. Lett.*, *30*(2), 1031, doi:10.1029/2002GL016178.

Santolik, O., D. A. Gurnett, J. S. Pickett, M. Parrot, and N. Cornilleau-Wehrlin (2003), Spatio-temporal structure of storm-time chorus, *J. Geophys. Res.*, *108*(A7), 1278, doi:10.1029/2002JA009791.

Santolik, O., D. A. Gurnett, J. S. Pickett, M. Parrot, and N. Cornilleau-Wehrlin (2004), A microscopic and nanoscopic view of storm-time chorus on 31 March 2001, *Geophys. Res. Lett.*, *31*, L02801, doi:10.1029/2003GL018757.

Santolik, O., D. A. Gurnett, J. S. Pickett, M. Parrot, and N. Cornilleau-Wehrlin (2005), Central position of the source region of storm-time chorus, *Planet. Space Sci.*, *53*, 299–305, doi:10.1016/j.pss.2004.09.056.

Santolik, O., D. A. Gurnett, J. S. Pickett, M. Parrot, and N. Cornilleau-Wehrlin (2006), Five years of investigation of whistler-mode chorus using the measurements of the Cluster spacefleet, in *Proceedings of the Cluster and Double Star Symposium—5th Anniversary of Cluster in Space*, edited by K. Fletcher, *Eur. Space Agency Spec. Publ., ESA-SP 598*, 53.1.

Sazhin, S. S., and M. Hayakawa (1992), Magnetospheric chorus emissions: A review, *Planet. Space Sci.*, *40*, 681–697, doi:10.1016/0032-0633(92)90009-D.

Scarf, F. L., D. A. Gurnett, W. S. Kurth, and R. L. Poynter (1982), Voyager 2 plasma wave observations at Saturn, *Science*, *215*, 587–594, doi:10.1126/science.215.4532.587.

Scarf, F. L., D. A. Gurnett, W. S. Kurth, and R. L. Poynter (1983), Voyager plasma wave measurements at Saturn, *J. Geophys. Res.*, *88*, 8971–8984, doi:10.1029/JA088iA11p08971.

Scarf, F. L., L. A. Frank, D. A. Gurnett, L. J. Lanzerotti, A. Lazarus, and E. C. Sittler Jr. (1984), Measurements of plasma, plasma waves and suprathermal charged particles in Saturn's inner magnetosphere, in *Saturn*, edited by T. Gehrels, pp. 318–353, Univ. of Ariz. Press, Tucson.

Shawhan, S. D. (1970), The use of multiple receivers to measure the wave characteristics of very-low-frequency noise in space, *Space Sci. Rev.*, *10*, 689–736, doi:10.1007/BF00171552.

Storey, L. R. O. (1953), An investigation of whistling atmospherics, *Philos. Trans. R. Soc. London, Ser. A*, *246*, 113–141, doi:10.1098/rsta.1953.0011.

Summers, D., B. Ni, and N. P. Meredith (2007), Timescales for radiation belt electron acceleration and loss due to resonant wave-particle interactions: 1. Theory, *J. Geophys. Res.*, *112*, A04206, doi:10.1029/2006JA011801.

Tsurutani, B. T., and E. J. Smith (1974), Postmidnight chorus: A substorm phenomenon, *J. Geophys. Res.*, *79*, 118–127, doi:10.1029/JA079i001p00118.

Tsurutani, B. T., and E. J. Smith (1977), Two types of magnetospheric ELF chorus and their substorm dependence, *J. Geophys. Res.*, *82*, 5112–5128, doi:10.1029/JA082i032p05112.

Tsurutani, B. T., E. J. Smith, H. I. West Jr., and R. M. Buck (1979), Chorus, energetic electrons and magnetospheric substorms, in *Wave Instabilities in Space Plasma*, edited by P. J. Palmadesso and K. Papadopoulos, pp. 55–62, D. Reidel, Dordrecht, Netherlands.

T. F. Averkamp, D. A. Gurnett, G. B. Hospodarsky, W. S. Kurth, and J. D. Menietti, Department of Physics and Astronomy, University of Iowa, Iowa City, IA 52242, USA. (george-hospodarsky@uiowa.edu)

M. K. Dougherty, Blackett Laboratory, Department of Space and Atmospheric Physics, Imperial College London, London SW7 2BZ, UK.

O. Santolik, Faculty of Mathematics and Physics, Charles University, KEVF MFF, V Holesovickach 2, Prague 8, CZ-18000, Czech Republic.